Start-Up Control of an Offshore Integrated MMC Multi-Terminal HVDC System With Reduced DC Voltage

Puyu Wang, *Student Member, IEEE*, Xiao-Ping Zhang, *Senior Member, IEEE*, Paul F. Coventry, and Ray Zhang

***Abstract*—The modular multilevel converter (MMC) provides promising development for high-voltage direct current (HVDC) applications, including multiterminal HVDC (MTDC) and renewable energy integration. This paper, considering an offshore wind farm (OWF) integrated MMC MTDC system, investigates its start-up process with three main developments: 1) it further develops the mathematical model of MTDC with active networks and proposes a hierarchical start-up control scheme; 2) for the terminal which connects the OWF, it proposes a reduced dc voltage control scheme of mitigating the current surges with deblocking the converter at zero voltage difference on submodules (SMs) and proposes an overall sequential start-up control scheme for the offshore integrated MTDC; and 3) it analyzes and compares different start-up control schemes. To evaluate the proposed sequential start-up control scheme, an offshore MMC HVDC system is established on the RTDS. The simulation results verify effectiveness of the proposed scheme on the MMC MTDC system with two control paradigms, i.e., master–slave control and droop control, respectively. In comparison with different start-up control schemes, the superiority of the mitigation of voltage spikes and current surges are shown using the proposed scheme with less complexity and easier implementation.**

***Index Terms*—Droop control, master–slave control, modular multilevel converter (MMC), multiterminal HVDC (MTDC), offshore wind farm (OWF), sequential start-up control.**

NOMENCLATURE

Tn	Terminal n$(\mathrm{n} = 1, \ldots, \mathrm{n})$.
CB	Circuit breaker.
SM	Submodule.
VSC	Voltage-source converter.
MMC	Modular multilevel converter.
OWF	Offshore wind farm.
PCC	Point of common coupling.
DFIG	Doubly fed induction generator.
HVDC	High-voltage direct current.
MTDC	Multiterminal HVDC.
RTDS	Real-time digital simulator.

Manuscript received December 07, 2014; revised March 25, 2015, July 02, 2015; accepted July 29, 2015. Date of publication September 03, 2015; date of current version May 02, 2016. This work was supported in part by EPSRC under Grant EP/K006312/1, National Grid, U.K., and the School of EESE, University of Birmingham. Paper no. TPWRS-01669-2014.

P. Wang and X. P. Zhang are with the School of Electronic Electrical and Systems Engineering, University of Birmingham, Birmingham, U.K. B15 2TT (e-mail: x.p.zhang@bham.ac.uk).

P. F. Coventry and R. Zhang are with National Grid, National Grid House, Warwick, U.K., CV34 6DA.

Color versions of one or more of the figures in this paper are available online at http://ieeexplore.ieee.org.

Digital Object Identifier 10.1109/TPWRS.2015.2466600

I. INTRODUCTION

WITH extensive research and applications, VSC technology has gradually achieved a high degree of maturity [1]–[3], and there has been numerous projects on VSC-based HVDC applications [4]–[10], including the applications of MTDC [5]–[8] and renewable energy integration in recent years [8]–[10]. There has been a variety of topologies with the VSC development [11]–[13]. Among them, one of these, the MMC, has salient features and shows its strong competitiveness, which has been well recognized by research and applications. Since there are a number of energy capacitors in the SMs of the MMCs, it is important to precharge these capacitors during the startup stage and the system startup control is essential.

In [14], a startup control scheme for the MMC was proposed. The proposed control scheme was based on the control of an auxiliary voltage source at the MMC dc-side. However, it is generally expected to start a system without auxiliary sources, which saves space and costs. In [15], a startup technique using additional resistors was proposed. The resistors were connected on the converter arms and were inserted/bypassed to limit the arm current. However, the additional resistive losses were not expected. In [16], a startup scheme with a two-stage charging process for MMC was proposed. Although the proposed charging scheme seemed to achieve charging the voltage of each SM capacitor to the rated value without auxiliary dc source, it had two main problems. First, in the first charging stage, the dc voltage was assumed to be the rated value and the charging of the SM capacitors was from the dc side. Under this assumption, the proposed scheme was only valid for the MMC under inverter operations. Second, in the second charging stage, the proposed scheme was that the SM capacitor voltages were charged to the rated value when the SMs were deblocked. However, the main objective of the start-up control of MMC is to pre-charge the SM capacitors to the rated value before they are deblocked. A start-up scheme for MMC HVDC was proposed in [17], including the calculation of the limiting resistance, the setting of the rising slope of dc voltage and the reference setting of reactive power. In [18], a calculation method for

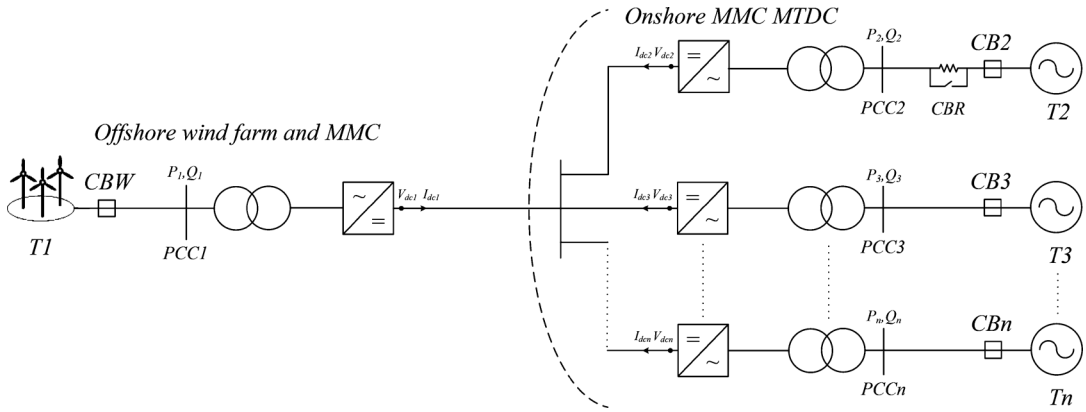

Fig. 1. MMC MTDC system with the integration of an OWF.

the minimum limiting resistance was proposed. In [19], the dynamics of the SMs in the MMC during the pre-charging process were analyzed and an optimized modulation algorithm was proposed for reducing the current surges when deblocking the MMC. Theoretically, an MMC can be deblocked at zero voltage difference and the current surges under this condition are the smallest. However, the control scheme proposed in [19] did not achieve zero voltage difference when deblocking the MMC. The start-up schemes proposed above were all based on two-terminal MMC HVDC systems.

In [20], a three-terminal MMC HVDC system based on a real application was investigated, and a control procedure of starting the system was proposed in detail. However, these procedures were obtained as a conceptual approach, which was based on the analysis at systematic level. There was no analysis on the dynamics of the SMs in the MMC with no comprehensive simulation results. Different sequential startup control was compared in [21], while most comparisons were based on simulations and the analysis were not comprehensive with no mathematical derivations. Hence, the startup control including the startup sequence of MMC MTDC systems deserves our study and exploration.

This paper investigates the start-up process of an OWF integrated MMC MTDC system with the main contributions given as follows.

1) Regarding an MMC MTDC system with active ac networks, the mathematical model before and after the deblocking of the converter is further developed on [19] into a second-order circuit with the consideration of the converter arm inductor. A hierarchical start-up control scheme is proposed. Considering the fact that an OWF is a passive ac network before the completion of its start-up, a start-up control strategy for the converter connecting with the OWF with deblocking the converter at zero voltage difference on SMs is proposed;
2) A four-terminal MMC HVDC system is established on the RTDS with one terminal connecting with an OWF. The effectiveness of the proposed sequential start-up control scheme is verified by the simulation results. The superiority of the proposed scheme, in terms of mitigating the voltage spikes and current surges, than other control schemes is compared, and the easy implementation of the proposed scheme is presented;
3) The proposed start-up control scheme is validated on the MMC MTDC system with master–slave control and droop control, respectively.

The remainder of this paper is organized as follows. Section II presents the structure of an MMC MTDC system and the basic control strategy. Section III further develops the mathematical model for the onshore MMC MTDC system before and after the deblocking of the converter, and proposes a hierarchical start-up control scheme. Section IV proposes a reduced dc voltage control scheme for the offshore connected converter, which is deblocked at zero voltage difference on SMs, and proposes an overall sequential start-up control scheme. The simulation results using RTDS are demonstrated in Section V. Further discussions on the subject are discussed in Section VI. Conclusions are presented in Section VII.

II. Basic Structure and Control Strategy

A. Basic Structure

Fig. 1(a) shows a single-line schematic diagram of an MMC MTDC system with the integration of an OWF. Both the offshore and onshore MMCs connect to the ac power sources, either the OWF or ac utility grids, through a three-phase transformer. The MTDC network can be in either radial or meshed arrangement. For the sake of simplicity, the MTDC investigated in this paper is in radial connection only. In Fig. 1(a), $\mathrm{T}n(n = 1, \ldots, n)$ denotes each terminal of the MTDC system; $\mathrm{CB}n(\mathrm{n} = 1, \ldots, \mathrm{n})$ denotes the AC circuit breaker at each terminal; $\mathrm{PCC}n\ (\mathrm{n} = 1, \ldots, \mathrm{n})$ denotes the common connecting point of the ac network.

Fig. 2 depicts the structure of one MMC and one SM within the MMC. Each MMC consists of three parallel-connected phase units where each phase unit comprises two arms. Each arm is composed of one arm inductor and n series-connected, identical half-bridge SMs. The arm inductor is designed to provide current control and limit the circulating current within the arm and to limit fault currents. A SM has three switching states, block (BLK), ON, and OFF. The SM is blocked either in the standby mode or under fault conditions. Under nominal conditions, each SM is either switched ON or OFF. In the ON state, the upper IGBT (S1) is switched on and the lower one (S2) is switched off, the voltage of the SM equals to the capacitor voltage ($V_{\mathrm{SM}} = V_C$). In the OFF state, S1 is switched

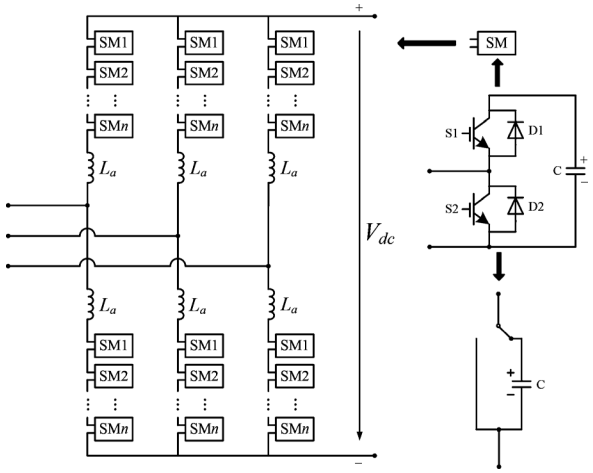

Fig. 2. Structure of one MMC and a SM.

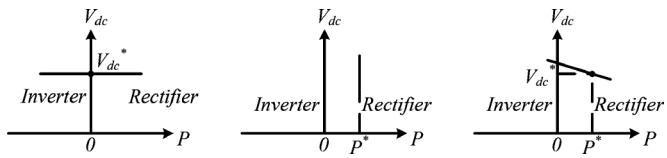

Fig. 3. Characteristics of dc voltage versus active power in MTDC. (a) Constant dc voltage control. (b) Constant active power control. (c) Droop control.

off and S2 is switched on, the capacitor is bypassed ($V_{\rm SM} = 0$). At the initial stage before the start-up of the system, the MMC is in standby mode with all SMs being blocked.

B. Control Strategy

The MTDC investigated in this paper is a four-terminal MMC HVDC system. For the offshore terminal, T1, the active power transferred is determined by the control of the DFIG-based OWF. Hence, MMC-1 applies ac voltage and frequency control [9] to stabilize the voltage magnitude and frequency at PCC1. For the onshore MTDC terminals, the MMCs are connected with active AC networks which can provide stable ac voltage at the PCC and active power to the connected MMC. The well-known *dq* decoupled control is applied. For MMC MTDC systems, two main control paradigms, i.e., master–slave control [22]–[24] and droop control [25]–[27], are generally used. For the master–slave control, one terminal is operated as the master terminal with constant dc voltage control, while the other terminals are operated as slave terminals with constant active power control. For the droop control, active power can be shared among different HVDC terminals. The characteristics of dc voltage versus active power in an MTDC are illustrated in Fig. 3. The following analysis on the start-up control will be conducted based on the system with master–slave control in which T2 is operated as the master terminal, while the other three terminals are operated as slave terminals. Reactive power control is applied by T2, T3 and T4 to control the reactive power at 0. The control strategy of each terminal is shown in Table I. The proposed start-up control will be validated on the system with master-slave control and droop control, respectively, in the case studies.

At the initial state, all of the capacitors within the MMCs are not charged and the voltage of the MTDC system is not established. During the period from the initial state to the steady state, in order to realize the start-up of the MTDC with small voltage spikes and current surges, the start-up process is divided into several stages rather than starting all terminals simultaneously.

- For T1, the start-up of the OWF necessitates a stable nominal AC voltage at PCC1. The establishment of the AC voltage relies on the inverted control of MMC-1 of the DC voltage. Hence, the start-up of T1 should be initiated after the start-up of T2 with a well-stabilized MTDC voltage.
- As for T2, it not only stabilizes the MTDC voltage, but also acts as a dc slack bus to balance the active power of the MTDC system. The active power transferred at T2 should be within its maximum rating. If the active power flow is not well regulated during the start-up period and is significantly over its transfer capability, it may affect the stabilization of the DC voltage controlled at T2 and there will be subsequent impact on the system performance. In addition, T1 with OWF is a weaker network compared with T3 and T4 with active ac networks. Hence, the coordinated start-up sequence plays a significant role in the start-up of the system and needs to be comprehensively investigated.

The start-up of the onshore MTDC system and the offshore terminal is analyzed in Sections III and IV, respectively.

TABLE I
CONTROL STRATEGY OF THE MTDC WITH MASTER–SLAVE CONTROL

Offshore MMC	**Control Strategy**	
MMC-1	V_{ac}, f	
Onshore MMC	***d*-axis**	***q*-axis**
MMC-2	V_{dc}	Q
MMC-3	P	Q
MMC-4	P	Q

III. MATHEMATICAL MODEL FOR THE ONSHORE MTDC DURING THE START-UP STAGE

A. Before the Deblocking of the MMCs

For the active ac network connected terminal, before deblocking the MMC, the ac circuit breaker is closed to provide initial charging for the SM capacitors. At BLK state, the MMC is operated under free-wheeling diodes as shown in Fig. 4 [19]. Considering the losses of the diodes and circuit resistors, the initial charging state of the MMC and its AC side can be illustrated as Fig. 5(a). It can be simplified to a RLC circuit, as shown in Fig. 5(b), where $R_{\rm eq} = 2R_s + 2nR_d$, $L_{\rm eq} = 2L_s + 2L_a$, $C_{\rm eq} = C/n$, $U_0 = \hat{u}_l$.

Before deblocking of the MMC, it is a second-order RLC circuit. Hence, its zero-state response can be derived after closing the AC circuit breaker. According to the Kirchhoff's voltage law (KVL), we have

$$u_R + u_L + u_C = U_0 \tag{1}$$

where $u_R = R_{\rm eq} \cdot i$, $u_L = L_{\rm eq}\frac{di}{dt}$

Substituting into (1), we have

$$R_{\rm eq} \cdot i + L_{\rm eq}\frac{di}{dt} + u_C = U_0. \tag{2}$$

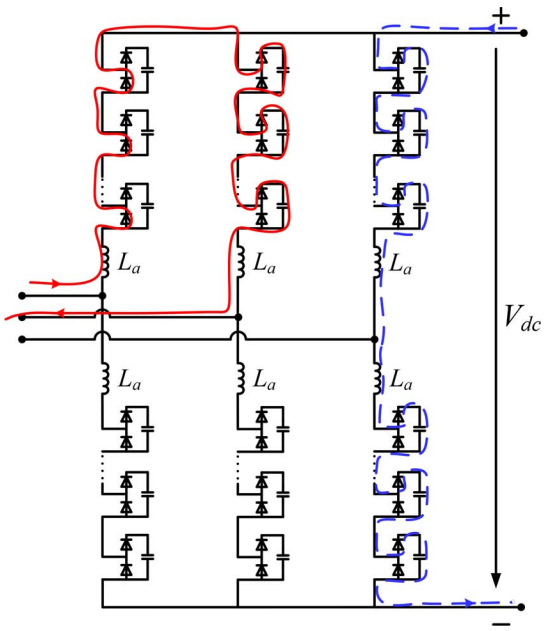

Fig. 4. MMC with BLK state.

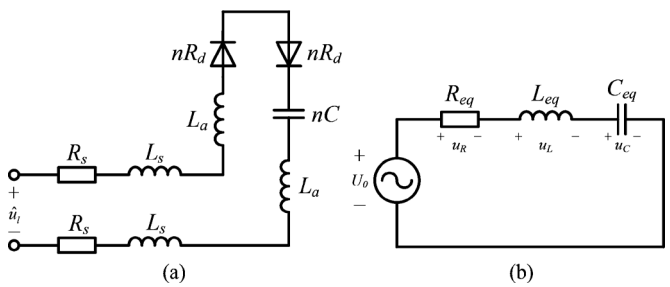

Fig. 5. Equivalent circuit before the deblocking the MMC. (a) Equivalent circuit. (b) Simplified circuit.

Since $i = C_{\rm eq}(du_c)/(dt)$, (2) can be written as

$$R_{\rm eq}C_{\rm eq}\frac{du_C}{dt} + L_{\rm eq}C_{\rm eq}\frac{d^2u_C}{dt^2} + u_C = U_0. \tag{3}$$

Considering the initial state of the circuit when closing the ac circuit breaker, we have

$$i_L(t_{0+}) = i_L(t_{0-}) = i(t_0) = 0$$
$$u_c(t_{0+}) = u_c(t_{0-}) = u_c(t_0) = 0.$$

The expression of u_C is

$$u_C = A_1e^{p_1t} + A_2e^{p_2t} + U_0 \tag{4}$$

where

$$p_{1,2} = -\delta \pm \sqrt{\delta^2 - \omega_0^2}, \quad \delta = \frac{R_{\rm eq}}{2L_{\rm eq}}, \quad \omega_0 = \frac{1}{\sqrt{L_{\rm eq}C_{\rm eq}}}$$
$$A_1 = -\frac{p_2U_0}{p_2 - p_1}, \quad A_2 = \frac{p_1U_0}{p_2 - p_1}.$$

Therefore, the final voltage of the SM capacitor of the MMC connected with an active ac network before deblocking of the MMC is $(u_c(t_\infty))/(n) = (U_0)/(n) = (\hat{u}_l)/(n)$.

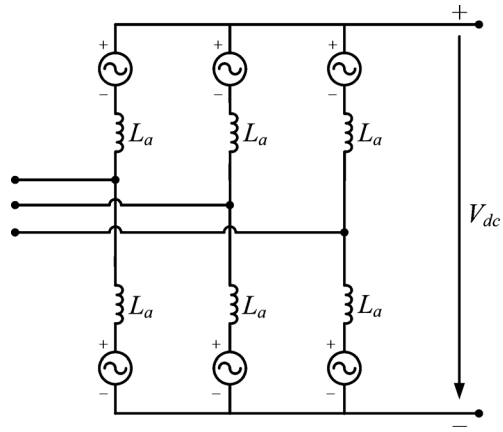

Fig. 6. Equivalent representation of MMC after deblocking.

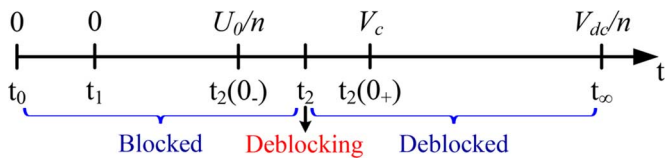

Fig. 7. Voltage change of an SM from the initial state of the MMC with an active ac network.

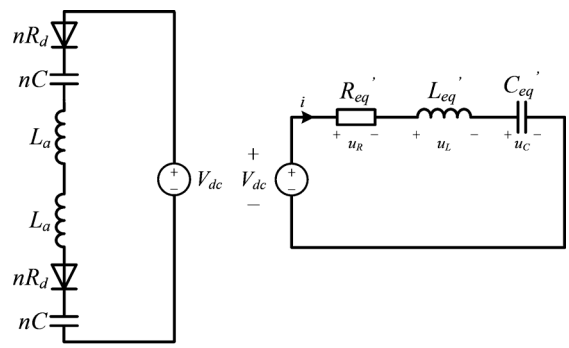

Fig. 8. Equivalent circuit before the deblocking MMC-1. (a) Equivalent circuit. (b) Simplified circuit.

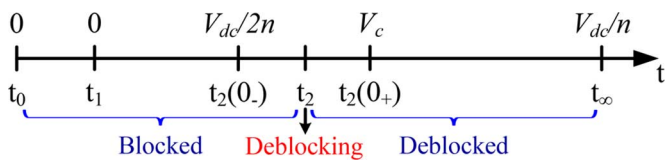

Fig. 9. Voltage change of a SM from the initial state of the MMC with a passive ac network.

B. After the Deblocking of the MMCs

After deblocking the MMC, the SMs on the converter arm can be regarded as a controllable ac voltage source [28], as shown in Fig. 6. When the system reaches the steady state, the nominal voltage of each SM capacitor is V_{dc}/n. The voltage change of a SM from the initial to the steady state is illustrated in Fig. 7. During the start-up process, the most significant voltage spikes and current surges are generated at t_2, which is the instant of deblocking the MMC. It is because of the voltage difference at $t_2(0_-)$ and $t_2(0_+)$. In order to mitigate this impact, the dc voltage reference is initially set at U_0 at t_2, so that the control system of the MMC will control the voltage of each SM equals to U_0/n, which equals to the SM final voltage before deblocking, and thus realize zero voltage difference at t_2.

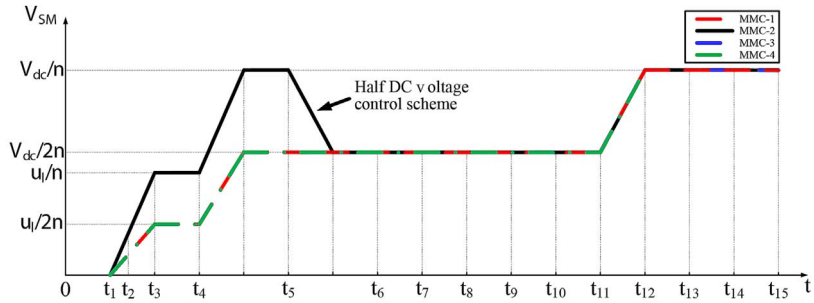

Fig. 10. Characteristics of SM capacitor voltages using the proposed sequential start-up control.

After deblocking the MMC, the dc voltage reference can be gradually increased to the nominal value.

C. Hierarchical Start-Up Control Scheme

Based on the previous analysis, a hierarchical start-up control scheme for the MMC terminal with active ac network is proposed.

Step 0: Initially, set the dc voltage reference to U_0.
Step 1: At t_1, close the ac circuit breaker and charge the voltage of the SM capacitor to U_0/n;
Step 2: At t_2, deblock the MMC;
Step 3: When the dc voltage is stably controlled at U_0, ramp the dc voltage reference to the nominal value to complete the start-up.

IV. Mathematical Model for the Offshore Terminal During the Start-Up Stage

A. Before the Deblocking of the MMC

At the initial stage when the wind farm has not been started, the wind farm connected terminal cannot provide stable ac voltage or inertia and is considered as a passive network. Under this condition, the SMs of the wind farm connected MMC can only be charged from the dc side, as the dashed line shown in Fig. 4.

When the voltage of the MTDC is stabilized by the control of MMC-2, the blocked MMC-1 is also equivalent to a RLC circuit, as shown in Fig. 8, where

$$R_{\mathrm{eq}}^{'} = 2nR_d, L_{\mathrm{eq}}^{'} = 2L_a, C_{\mathrm{eq}}^{'} = C/2n.$$

Since there are *2n* SM capacitors connected in series, each capacitor will be finally charged to $V_{dc}/2n$.

B. After the Deblocking of the MMC

The nominal voltage of each SM is V_{dc}/n. The voltage change of a SM from the initial to the steady state is illustrated in Fig. 9. If the wind farm connected MMC is deblocked directly, there must be a current surge due to the SM voltage difference at the deblocking instant. Therefore, in order to reduce the voltage difference at the deblocking stage, the controlled dc voltage is regulated to a reduced value, which is named as reduced dc voltage control scheme. According to the derivation in Section IV-A, the SM voltage difference becomes zero when the dc voltage is reduced to half of its rated value. In this paper, the half DC voltage control scheme is applied. Hence, the reference of the dc voltage at T2, after being set at the nominal value, is reduced to $V_{\mathrm{dc}}/2$ prior to the deblocking of MMC-1.

C. Sequential Start-Up Scheme

Based on the previous analysis on the start-up control of the active and passive network connected MMCs, an efficient sequential start-up control scheme for an offshore integrated MMC MTDC system is proposed as follows.

Step 0 (t_0): Initially, set $V_{\mathrm{dcref}} = u_l$, $V_{\mathrm{acref}} = 0$, $P_{3\mathrm{ref}} = P_{4\mathrm{ref}} = 0$;
Step 1 (t_1): Close *CB2*;
Step 2 (t_2): Close *CBR*;
Step 3 (t_3): When the SM capacitor voltages of MMC-2 are charged to $\hat{u}_l$, deblock MMC-2;
Step 4 (t_4): When the DC voltage is controlled at $\hat{u}_l$, set $V_{\mathrm{dcref}} = V_{\mathrm{dc}}^*$;
Step 5 (t_5): When the DC voltage is stabilized at V_{dc}^* and the SM capacitor voltages of T1, T3 and T4 are charged to $V_{\mathrm{dc}}^*/2n$, set $V_{\mathrm{dcref}} = V_{\mathrm{dc}}^*/2$.
Step 6 (t_6): When the DC voltage is stabilized at $V_{dc}^*/2$, deblock MMC-1;
Step 7(t_7): Close *CB3*;
Step 8 (t_8): Close *CB4*;
Step 9 (t_9): Since the SM capacitor voltages of MMC-3 and MMC-4 are $V_{dc}^*/2n$ and the DC voltage is controlled at $V_{dc}^*/2$, there will be no voltage difference when deblocking the MMCs. Deblock MMC-3;
Step 10 (t_{10}): Deblock MMC-4;
Step 11 (t_{11}): When the active power at T3 and T4 is well stabilized, set $V_{\mathrm{dcref}} = V_{\mathrm{dc}}^*$;
Step 12 (t_{12}): When the DC voltage is stabilized at V_{dc}^*, set $V_{\mathrm{acref}} = V_{\mathrm{ac}}^*$;
Step 13 (t_{13}): When the AC voltage at PCC1 is well stabilized at V_{ac}^*, close *CBW*;
Step 14 (t_{14}): Deblock the OWF;
Step 15 (t_{15}): Set $P_{3ref} = P_3^*$, $P_{4\mathrm{ref}} = P_4^*$.

When the active power of the MTDC reaches the nominal condition, the start-up of the whole system is completed.

During the start-up process, the characteristics of the SM capacitor voltage of each MMC are illustrated in Fig. 10. It can be seen that due to the effective sequential start-up control, the SM capacitor voltages gradually reach their nominal state. Moreover, the start-up sequence of each terminal is well coordinated to achieve minimum power losses. In order to clearly present the system performance at each control action in the case studies,

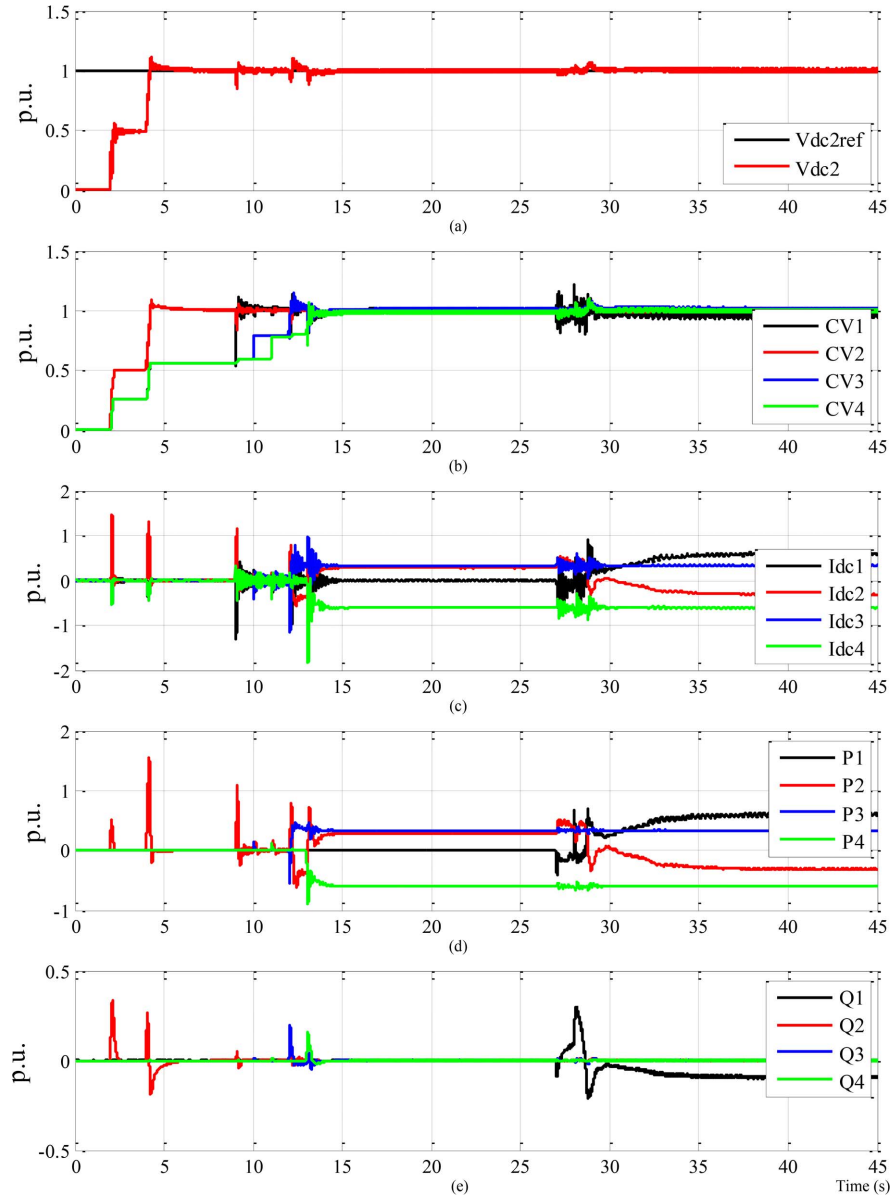

Fig. 11. MTDC without a starting resistor and without reduced DC voltage control (*Case A*): (a) MMC-2 DC side voltage, (b) SM capacitor voltages; (c) MTDC currents, (d) active power, and (e) reactive power.

the control action sequence and the delay between two sequential actions are shown in Table III.

V. RTDS Simulation System and Results

In order to verify the effectiveness of the proposed scheme, a four-terminal MMC HVDC system with one terminal connected with an OWF is established on the RTDS. The detailed system parameters are provided in Table II and the control strategy of each terminal is described in Section II-B.

Since the start-up control proposed by previous literature mainly relied on the use of starting resistors, in the case studies the start-up control of the MTDC with/without starting resistors and with/without reduced DC voltage control is compared. Four simulation cases are conducted.

- *In Case A, the MTDC is started without starting resistors and without reduced DC voltage control;*
- *Case B is similar to Case A, except that the MTDC is started with starting resistors;*
- *Case C is similar to Case B, except that the MTDC is started with reduced DC voltage control.*
- *Case D is similar to Case C, except that the MTDC uses droop control instead of master–slave control. Since the voltage droop control has been mainly used on the MTDC, the objective of Case D is to evaluate the proposed start-up sequence on the MTDC with droop control.*

A. Case A

In this case, the MTDC is started without starting resistor and without reduced dc voltage control. Simulation results are shown in Fig. 11. Fig. 11(a) shows the reference dc voltage (V_{dc2ref}) and the controlled dc voltage (V_{dc2}) of MMC-2; Fig. 11(b) shows the voltages of the SM capacitors, where CV_n ($n = 1, \ldots, 4$) denote the SM capacitor voltage of

TABLE II
PARAMETERS OF THE OFFSHORE INTEGRATED 4-T MMC HVDC SYSTEM

Parameters	VALUES	Comments
AC system voltage	240 kV	L-L, RMS
AC system inductance L_{AC}	150 mH	SCR = 8 at PCC
Transformer ratio	240 kV/30 kV	Y/Δ
Transformer leakage inductance	5%	
Wind turbine rated output	1.4 MW	
No. of wind turbines	60	
Wind farm rated output	84 MW	
DC bus voltage $V_{dc}/2$	50 kV	± 50 kV
MMC rating	150 MVA	
No. of SMs per arm	6	
Arm inductance L_a	3 mH	
SM capacitance C	2500 μF	
Diode resistance R_d	0.02 Ω	
T3 active power P_3^*	50 MW	Import to MTDC
T4 active power P_4^*	90 MW	Export from MTDC
Reactive power reference	0 MVar	T2, T3, T4

TABLE III
DESCRIPTION OF THE OPERATION TIME OF THE CONTROL SEQUENCE IN FIG. 10

t_n	Time	Description
t_0	0 s	Set $V_{dcref} = u_l$, $V_{acref} = 0$, $P_{3ref} = P_{4ref} = 0$
t_1	2 s	Close *CB2*
t_2	2.5 s	Close *CBR*
t_3	4 s	Deblock MMC-2
t_4	6 s	Set $V_{dcref} = V_{dc}^*$
t_5	8 s	Set $V_{dcref} = V_{dc}^*/2$
t_6	9 s	Deblock MMC-1
t_7	10 s	Close *CB3*
t_8	11 s	Close *CB4*
t_9	12 s	Deblock MMC-3
t_{10}	13 s	Deblock MMC-4
t_{11}	18 s	Set $V_{dcref} = V_{dc}^*$
t_{12}	21 s	Set $V_{acref} = V_{ac}^*$
t_{13}	27 s	Close *CBW*
t_{14}	28 s	Deblock OWF
t_{15}	29 s	Set $P_{3ref} = P_3^*$, $P_{4ref} = P_4^*$

each MMC; Fig. 11(c) shows the dc currents of the MTDC, where $\mathrm{I_{dcn}}$ $(\mathrm{n} = 1, \ldots, 4)$ denote the DC current at each terminal; Fig. 11(d) shows the active power of the MTDC, where $\mathrm{P_n}$ $(\mathrm{n} = 1, \ldots, 4)$ denote the active power measured at each terminal; Fig. 11(e) shows the reactive power of the MTDC, where $\mathrm{Q_n}$ $(\mathrm{n} = 1, \ldots, 4)$ denote the reactive power measured at each terminal. The measuring points of these quantities are illustrated in Fig. 1.

Fig. 11(c) demonstrates that, due to the absence of starting resistor, the DC current at T2 increases significantly when closing CB2. Since V_{dcref} is always set at V_{dc}^* during the start-up process, the voltages of the SM capacitors will be instantly controlled and increase to the reference value when the MMC is deblocked. If the MMC is deblocked at t, the voltage difference of the SM capacitor is not zero between $\mathrm{t}(0_-)$ and $\mathrm{t}(0_+)$, leading to the step rise of the voltages of the SM capacitors. This will causes large voltage spikes and current surges. According to Table III, the MMC at each terminal is deblocked at 4 s, 9 s, 12 s, and 13 s, and oscillations of the dc voltage and SM capacitor voltages can be observed in Fig. 11(a) and (b). The current surges and power oscillations can be observed at those 4 instants as shown in Fig. 11(c) and (d). In addition, since the dc voltage is controlled at V_{dc}^* at all times, after closing *CB3* and *CB4*, the MMC dc side voltage is much larger than the MMC ac side voltage, leading to the current injection from the MMC DC side to the ac side. According to the current direction and the BLK state of the MMC, this current will charge the SM capacitor, resulting in the voltage rise in the SM capacitor. Table III shows that *CB3* and *CB4* is closed at $\mathrm{t_6}$ and $\mathrm{t_7}$, respectively. Fig. 11(b) demonstrates the voltage rise of the SM capacitor in MMC-3 at 10 s and in MMC-4 at 11 s. This also leads to the oscillations on the dc voltage and dc current as shown in Fig. 11(a) and (c) at these two instants, as well as the oscillations on the active power as shown in 11(d).

B. Case B

In this case, the start-up sequence is similar to that of *Case A*, except that the starting resistor is used. Simulation results are shown in Fig. 12. Fig. 12(a) shows the reference dc voltage and controlled dc voltage of MMC-2; Fig. 12(b) shows the voltages of the SM capacitors; Fig. 12(c) shows the DC currents of the MTDC; Fig. 12(d) shows the active power of the MTDC; Fig. 12(e) shows the reactive power of the MTDC.

Due to the use of the starting resistor, the inrush current at T2 becomes smaller when closing CB2 at 2 s. In order to visibly compare the current rise between *Case A* and *Case B*, the DC currents at T2 of both cases are shown in Fig. 13.

The DC current at T2 in *Case A* rises to 1.5 p.u., which is 1.5 times larger than that in *Case B*. Hence, the use of starting resistor is important and can effectively limit the inrush current during start-up period.

C. Case C

In this case, the start-up sequence is similar to that of *Case B*, except that the reduced dc voltage control is applied, that is to say, the proposed sequential start-up control is applied. Simulation results using the proposed sequential start-up scheme are shown in Fig. 14. Fig. 14(a) shows the reference dc voltage and controlled dc voltage of MMC-2; Fig. 14(b) shows the voltages of the SM capacitors; Fig. 14(c) shows the dc currents of the MTDC; Fig. 14(d) shows the active power of the MTDC; Fig. 14(e) shows the reactive power of the MTDC.

Fig. 14(a) shows that the dc voltage controlled at T2 well traces the voltage reference after deblocking the converter with few oscillations. Fig. 14(b) demonstrates the voltages of the SM capacitors, which are generally the same as the diagram drawn in Fig. 10 based on previous analysis and have smaller voltage spikes than those in *Case A* and *Case B* at the MMC deblocking instants. Fig. 14(c) shows that the performance of the dc currents has smaller current surges in comparison to those in *Case A* and *Case B*, since the MMCs are all deblocked with zero voltage difference. The performance of the active power has small oscillations and well traces its predefined reference setting as shown in Fig. 14(d). The oscillations of the reactive power are relatively small as shown in Fig. 14(e). Due to the effective sequential start-up control, each terminal is started and reaches

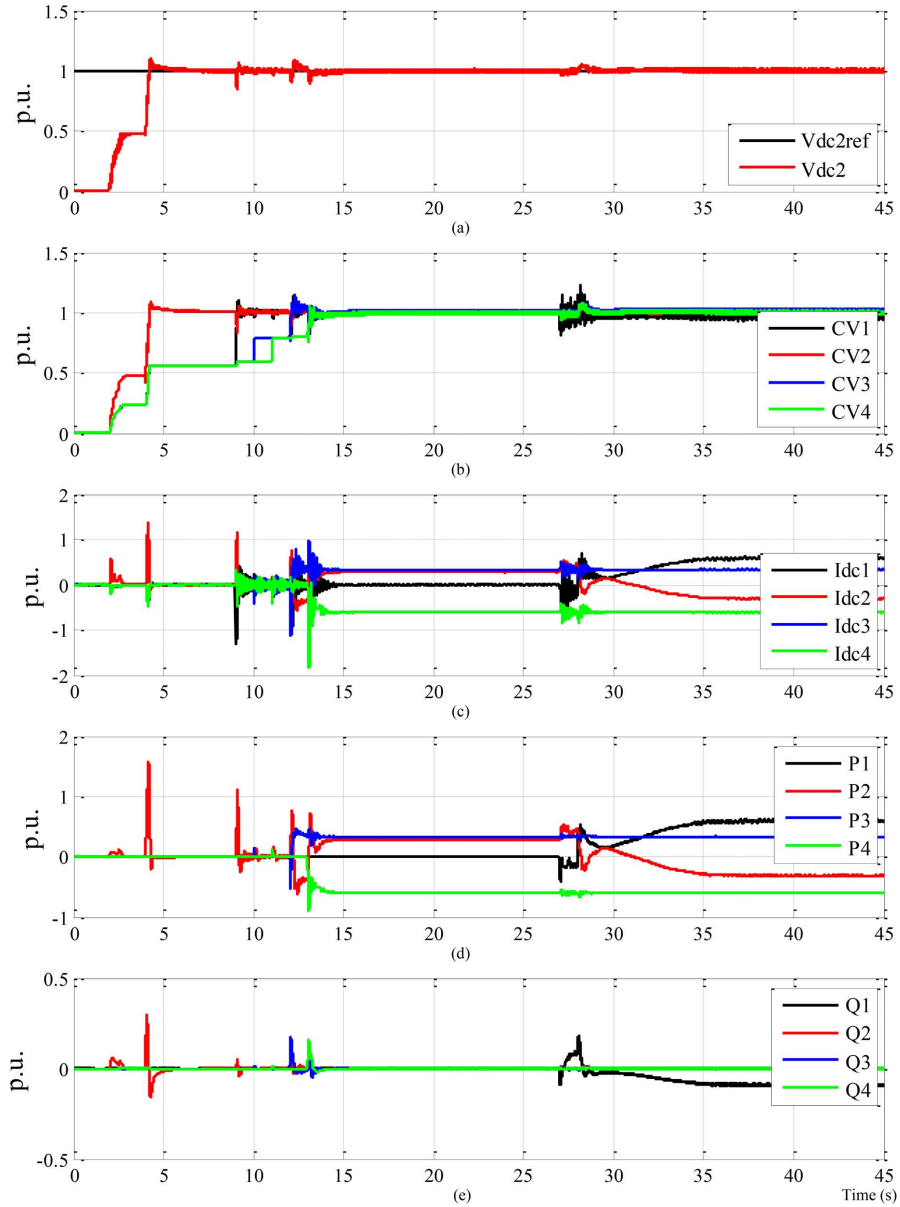

Fig. 12. MTDC with a starting resistor and without reduced DC voltage control (*Case B*). (a) MMC-2 dc side voltage. (b) SM capacitor voltages. (c) MTDC currents. (d) Active power. (e) Reactive power.

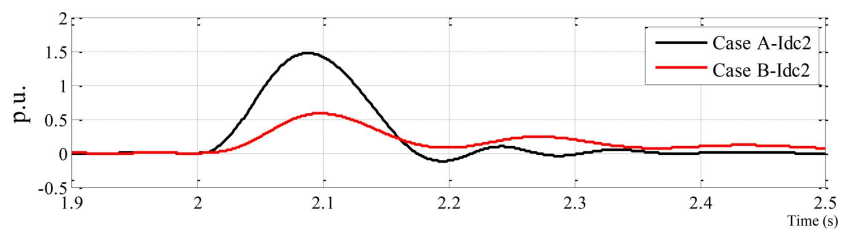

Fig. 13. Comparisons of the dc current at T2 of *Case A* and *Case B*.

its reference setting in sequence, which enables the completion of the start-up of the system with small voltage spikes and current surges. The simulation results demonstrate that *Case C* uses both starting resistors and reduced dc voltage control has minimum voltage spikes and current surges.

In order to visibly compare the performance with and without reduced dc voltage control, the capacitor voltage of MMC-1 of *Case B* and *Case C* is put together in Fig. 15(a) and the dc current at T1 of both cases is put together in Fig. 15(b). Fig. 15(c) shows a zoomed portion of Fig. 15(b). The performance using the start-up control sequence in *Case A* can be observed to be more stable with fewer voltage spikes as shown in Fig. 15(a) and smaller current surges, particularly when deblocking the MMCs, as shown in Fig. 15(b) and (c). Therefore,

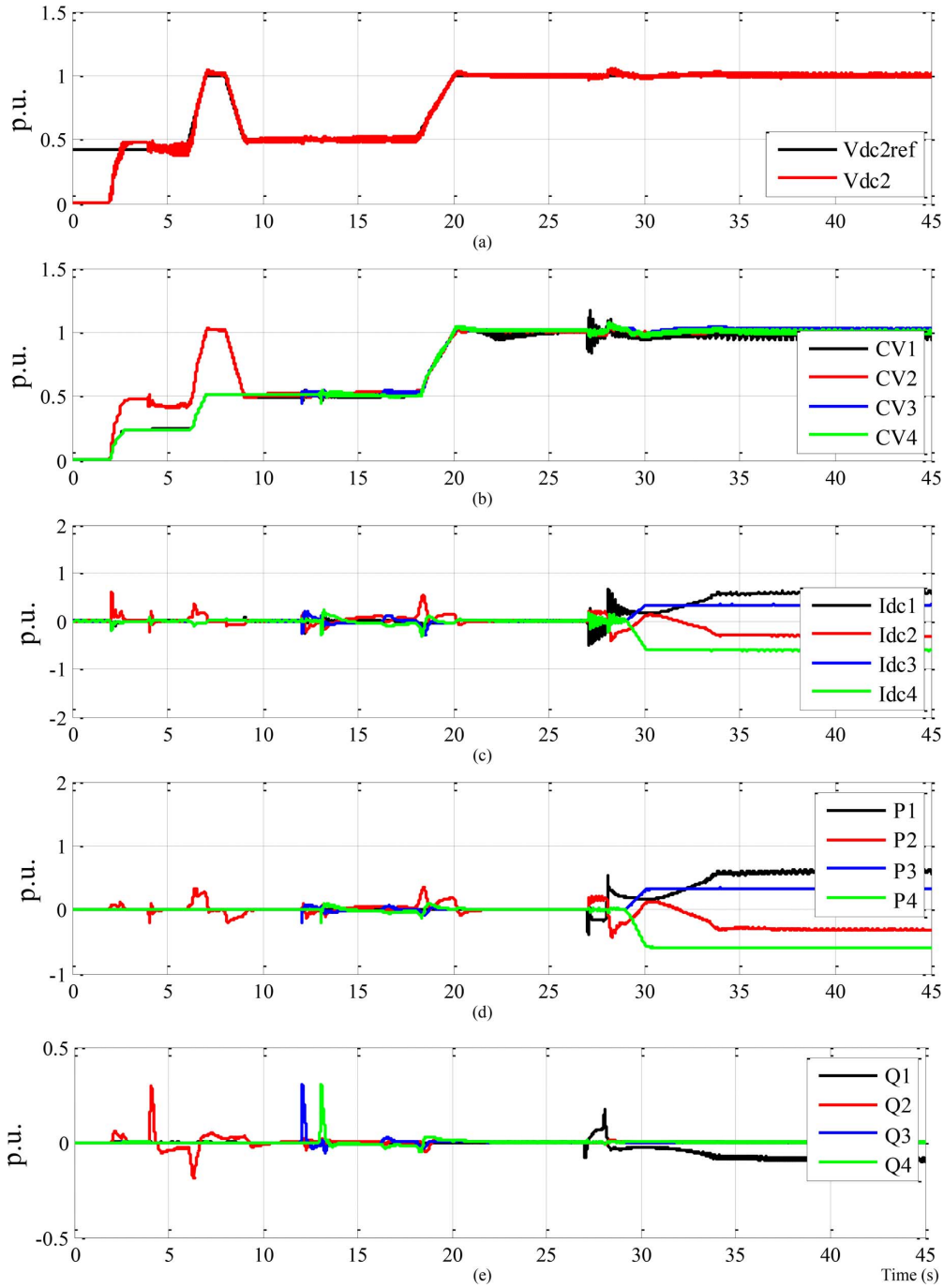

Fig. 14. MTDC with master-slave control using the proposed sequential start-up control (*Case C*). (a) MMC-2 dc side voltage. (b) SM capacitor voltages. (c) MTDC currents. (d) Active power. (e) Reactive power.

the proposed sequential start-up control scheme on the offshore integrated MMC MTDC system is considered to be more appropriate and can start the MTDC in a stable and smooth manner.

D. Case D

In order to evaluate the proposed start-up control scheme on the MMC MTDC system with droop control, in this case, T2, T3, and T4 apply voltage droop control. The dc voltage reference setting of T2 is the same as that of *Case C* and applies to the dc voltage reference settings of T3 and T4. The active power reference settings are the same as those of *Case C*. Simulation results are shown in Fig. 16. Fig. 16(a) shows the reference dc voltage and controlled dc voltage of MMC-2; Fig. 16(b) shows the voltages of the SM capacitors; Fig. 16(c) shows the dc currents of the MTDC; Fig. 16(d) shows the active power of the MTDC; Fig. 16(e) shows the reactive power of the MTDC.

The simulation results shown in Fig. 16 are similar to those in Fig. 16. Fig. 16(a) demonstrates that the dc voltage well traces the reference voltage. The voltage spikes of the SM capacitors in Fig. 16(b) are as small and comparable as those in Fig. 14(b). In *Case C*, master–slave control is used where T2 is operated as a dc slack bus, which is responsible for balancing the active power of the MTDC grid. In this case, since T2, T3 and T4 apply voltage droop control, the active power is shared

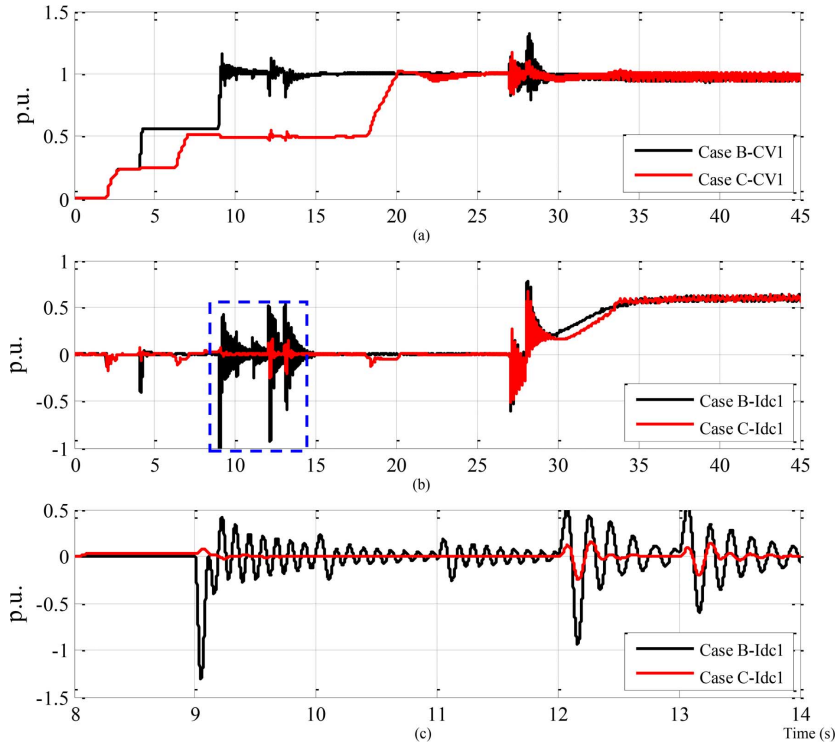

Fig. 15. Comparisons of the system performance of *Case B* and *Case C*. (a) One capacitor voltage of MMC-1. (b) DC current at T1. (c) Zoomed dc current at T1.

among these HVDC terminals. The performance of the dc current and active power at T2 can be observed to have fewer oscillations in Fig. 16(c) and (d) in comparison with those in Fig. 14(c) and (d). The simulation results indicate that the proposed sequential start-up control scheme is valid for the MMC MTDC system with droop control.

VI. Discussions

In *Case A* and *Case B*, although its performance is not as good as that of *Case C*, the overall start-up performance is acceptable with tolerable voltage spikes and current surges. This is due to the use of the sequential start-up control. If the system is started without considering any starting sequence, such as starting the terminal with active power control prior to the dc voltage controlled terminal or connecting the OWF when the ac voltage at the wind farm side has not been well stabilized, the performance may become much worse with significant overvoltage and overcurrent and there may be difficulty in integrating the OWF.

In *Case D*, it is observed that the proposed start-up control is also valid for the MMC MTDC system with droop control and the performance is similar to that of *Case C*. Thanks to the application of voltage droop control, the active power can be shared among different HVDC terminals. In comparison to *Case C*, the performance of the active power shown in *Case D* has fewer oscillations.

The proposed sequential start-up control scheme for the offshore integrated MMC MTDC system can largely mitigates the voltage spikes and current surges with zero SM voltage difference at the deblocking of the MMCs during the system start-up. In addition, the control methodology is easy to realize without complex strategies as shown in Table III. The intrinsic considerations are the sequence of each terminal and appropriate control of the regulated dc voltage, SM capacitor voltages, ac voltages at the PCCs and active power. The half dc voltage control scheme applied in this paper has requirement on the design of system parameters, which needs to be considered before the system commission. However, the reduced dc voltage control scheme with starting resistor can be applied in any MMC MTDC system and it largely reduces the impact on the voltage spikes and current surges at the deblocking of the MMCs due to the reduced voltage difference of SM capacitors. In addition, the delay between two sequential actions, i.e., t_k and t_{k+1} $(k = 1, \ldots, 13)$ shown in Fig. 10 and Table III can be further optimized to shorten the start-up process.

VII. Conclusion

This paper has investigated the start-up control of an OWF integrated MMC MTDC system. After the derivation and analysis of the mathematical models on both the active and passive networks connected MMCs, a hierarchical control scheme for the active network connected MMCs and a reduced dc voltage control scheme for the OWF connected MMC have been proposed. The combination of both schemes forms an overall sequential start-up control scheme. A four-terminal MMC HVDC system with one terminal connected with an OWF has been established on the RTDS. The system with either master-slave control or droop control can be well started using the proposed control scheme with small voltage spikes and current surges. In comparison with the start-up control schemes with/without starting resistor and half dc voltage control, the superiority of the proposed scheme has been observed. This paper has also discussed the potential development on the proposed scheme and the importance of the sequential start-up for the MTDC. The proposed sequential start-up control scheme has less complexity and is easy to realize. Although half dc voltage control scheme may

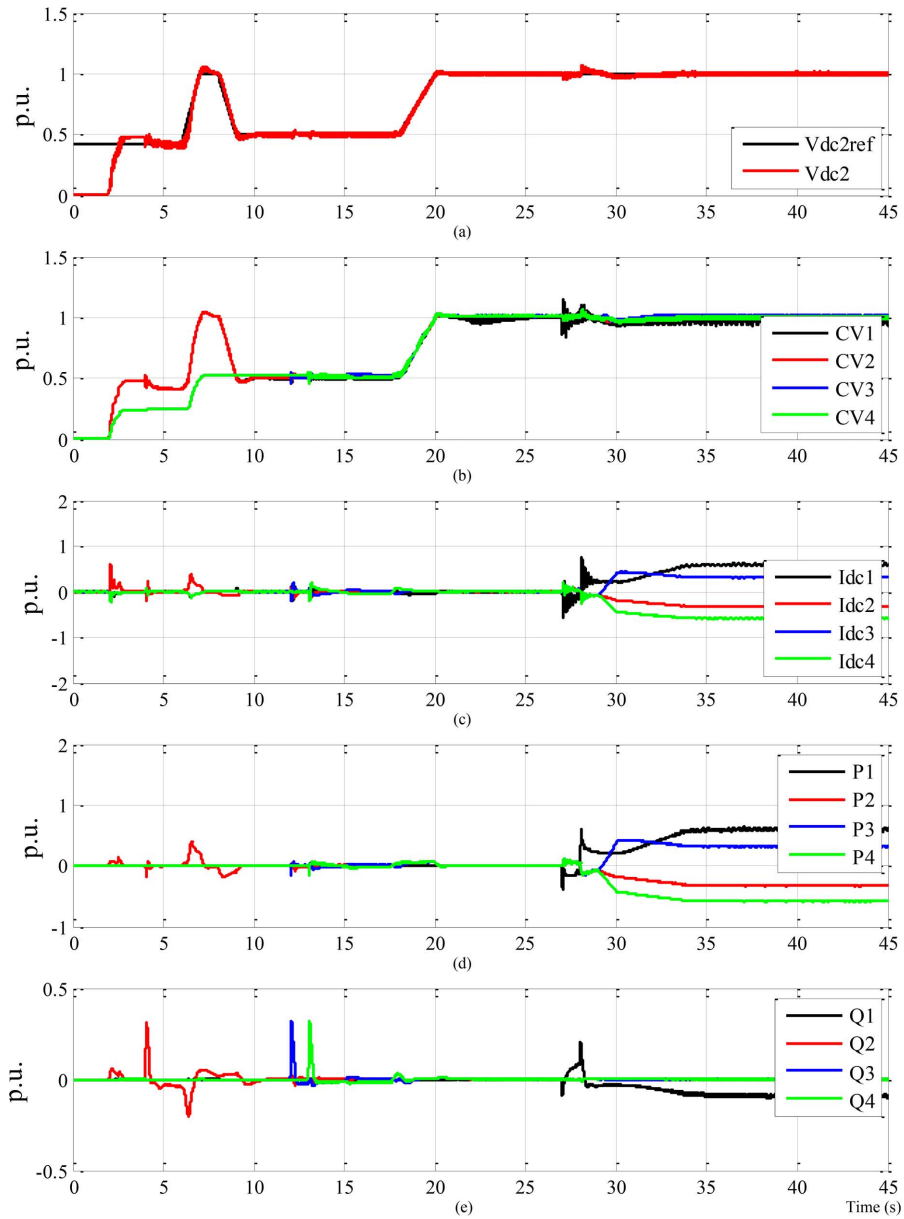

Fig. 16. MTDC with droop control using the proposed sequential start-up control (*Case D*). (a) MMC-2 dc side voltage. (b) SM capacitor voltages. (c) MTDC currents. (d) Active power. (e) Reactive power.

not be applicable for every MMC MTDC projects, the reduced dc voltage control scheme can be applied for all of them.

Appendix
Description of the Work in [19]

Since some of the contributions and development of this paper were based on [19]. The Appendix below provides an overview of the work in [19]:

Based on a two-terminal MMC HVDC, the pre-charging dynamic process of the converter is analyzed, so as to search a suitable pre-charging control strategy. Taking a single MMC station, the factors of causing transient over current during the deblocking action are analyzed. An optimized modulation algorithm is presented, making it suitable for both the pre-charging process. When the MMC-HVDC supplying for a passive network, the ac network of the active side will be the only energy source for MMCs. Based on the pre-charging control approach for a single MMC, a control strategy for both ends of MMC-HVDC is introduced, mitigating the problem of the capacitors undercharged. Finally, a simulation system is established and the simulation results verify the feasibility and validity of the control strategies mentioned.

References

[1] B. Anderson and C. D. Barker, "A new era in HVDC?," *Inst. Elect. Eng. Rev.*, vol. 46, no. 2, pp. 33–39, Mar. 2000.

[2] J. Dorn, H. Huang, and D. Retzmann, "A new multilevel voltage sourced converter topology for HVDC applications," in *Proc. CIGRE Session*, Paris, France, 2008, pp. 1–8.

[3] N. Flourentzou, V. Agelidis, and G. Demetriades, "VSC-based HVDC power transmission systems: An overview," *IEEE Trans. Power Electron.*, vol. 24, no. 3, pp. 592–602, Mar. 2009.

[4] H. Wang, G. Tang, Z. He, and J. Yang, "Efficient grounding for modular multilevel HVDC converters (MMC) on the AC side," *IEEE Trans. Power Del.*, vol. 29, no. 3, pp. 1262–1272, Jun. 2014.
[5] G. Bathurst and P. Bordignan, "Delivery of the Nan'ao multiterminal VSC-HVDC system," in *Proc. IET 11th Int. Conf. AC DC Power Transmission*, Feb. 2015, pp. 1–6.
[6] CIGRE Working Group B4.52, "Feasibility of HVDC grids," CIGRE Technical Brochure. Paris, Apr. 2013.
[7] T. K. Vrana, Y. Yang, D. Jovcic, S. Dennetiere, J. Jardini, and H. Saad, "The CIGRE B4 DC grid test system," *CIGRE Electra Mag.*, vol. 270, pp. 10–19, Oct. 2013.
[8] X. Chen, H. Sun, J. Wen, W.-J. Lee, X. Yuan, N. Li, and L. Yao, "Integrating wind farm to the grid using hybrid multiterminal HVDC technology," *IEEE Trans. Ind. Appl.*, vol. 47, no. 2, pp. 965–972, Mar./Apr. 2011.
[9] N. M. Kirby, L. Xu, M. Luckett, and W. Siepmann, "HVDC transmission for large offshore wind farms," *IEE Power Eng. J.*, vol. 16, no. 3, pp. 135–141, Jun. 2002.
[10] V. Hussennether, J. Rittiger, A. Barth, D. Worthington, G. Dell'Anna, M. Rapetti, B. Hhnerbein, and M. Siebert, "Projects BorWin2 and HelWin1—Large scale multilevel voltage-sourced converter technology for bundling of offshore windpower," in *Proc. CIGRE Session*, Paris, France, 2012, vol. B4-306.
[11] B. Andersen, L. Xu, P. J. Horton, and P. Cartwright, "Topologies for VSC transmission," *Power Eng. J.*, vol. 16, no. 3, pp. 142–150, Jun. 2002.
[12] J. Rodriguez, J.-S. Lai, and F. Z. Peng, "Multilevel inverters: A survey of topologies, controls, and applications," *IEEE Trans. Ind. Electron.*, vol. 49, no. 4, pp. 724–738, Aug. 2002.
[13] M. Davies, M. Dommaschk, J. Dorn, J. Liang, D. Retzmann, and D. Soerangr, "HVDC PLUS—Basics and principle of operation," Siemens, , Tech Rep., 2008.
[14] K. Li and C. Zhao, "New technologies of modular multilevel converter for VSC-HVDC application," in *Proc. Power Energy Eng. Conf.*, Mar. 2010, pp. 1–4.
[15] A. Das, H. Nademi, and L. Norum, "A method for charging and discharging capacitors in modular multilevel converter," in *Proc. IEEE Ind. Electron. Soc. Conf.*, 2011, pp. 1058–1062.
[16] K. Shi, F. Shen, D. Lv, P. Lin, M. Chen, and D. Xu, "A novel startup scheme for modular multilevel converter," in *Proc. IEEE Energy Convers. Congr. Expo.*, 2012, pp. 4180–4187.
[17] T. Li, C. Zhao, J. Xu, X. Cai, and C. Lin, "Start-up scheme for HVDC system based on modular multilevel converter," in *Proc. 2nd IET Renew. Power Gen. Conf.*, Sep. 2013, pp. 1–4.
[18] Y. Jiang, J. Hu, H. Song, M. Zhang, X. Wang, Z. Rao, G. Wang, and G. Zhu, "Study on start-up control strategies for HVDC-Flexible system based on MMC," in *Proc. Chinese Autom. Congress*, Nov. 2013, pp. 126–131.
[19] M. Kong, Y. Qiu, Z. He, W. He, and J. Liu, "Pre-charging control strategies of modular multilevel converter for VSC-HVDC," (in Chinese) *Power Syst. Tech.*, vol. 35, no. 11, Nov. 2011.
[20] X. Li, Z. Yuan, J. Fu, Y. Wang, T. Liu, and Z. Zhu, "Nanao multiterminal VSC-HVDC project for integrating large-scale wind generation," in *Proc. IEEE Power Energy Soc. Gen. Meeting Conf. Expo.*, Jul. 2014, pp. 1–5.
[21] P. Y. Wang, Z. Li, X. P. Zhang, and P. F. Coventry, "Start-up sequences of an offshore integrated MMC MTDC system," in *Proc. 11th IET Int. Conf. on AC and DC Power Transmission*, Feb. 2015.
[22] T. M. Haileselassie, "Control, dynamics and operation of multi-terminal VSC-HVDC transmission systems," Ph.D. dissertation, Dept. Electr. Power Eng., Norwegian Univ. Sci. Technol., Trondheim, Norway, 2012.
[23] J. Cao, W. Du, H. F. Wang, and S. Q. Bu, "Minimization of transmission loss in meshed AC/DC grids with VSC-MTDC networks," *IEEE Trans. Power Syst.*, vol. 28, no. 3, pp. 3047–3055, Aug. 2013.
[24] N. Yousefpoor, S. Kim, and S. Bhattacharya, "Multi-terminal DC grid control under loss of terminal station," in *Proc. IEEE Energy Conv. Congr. Expo.*, Sep. 2014, pp. 744–749.
[25] T. M. Haileselassie and K. Uhlen, "Power system security in a meshed north sea HVDC grid," *Proc. IEEE*, vol. 101, no. 4, pp. 978–990, Feb. 2013.
[26] C. Dierckxsens, K. Srivastava, M. Reza, S. Cole, J. Beerten, and R. Belmans, "A distributed DC voltage control method for VSC MTDC systems," *Elect. Power Syst. Res.*, vol. 82, no. 1, pp. 54–58, Jan. 2012.
[27] W. Wang and M. Barnes, "Power flow algorithms for multi-terminal VSC-HVDC with droop control," *IEEE Trans. Power Syst.*, vol. 29, no. 4, pp. 1721–1730, Jul. 2014.
[28] A. Antonopoulos, L. Angquist, and H. P. Nee, "On dynamics and voltage control of the modular multilevel converter," in *Proc. 13th Euro. Conf. Power Electron. Appl.*, Sep. 2009, pp. 1–10.

Puyu Wang (S'13) received the B.Eng. degrees from Huazhong University of Science and Technology (HUST), China, and the University of Birmingham, Birmingham, U.K., in 2011, both in electrical engineering. He is currently working toward the Ph.D. degree at the University of Birmingham, Birmingham, U.K.

He has been a Research Fellow with the University of Birmingham, Birmingham, U.K., since 2013. His research interests include VSC-HVDC technology, DC-DC converters, grid integration of renewable energy, and power electronics applications in power systems.

Xiao-Ping Zhang (M'95–SM'06) received the B.Eng., M.Sc., and Ph.D. degrees in electrical engineering from Southeast University, Nanjing, China in 1988, 1990, and 1993, respectively.

He is currently a Professor of electrical power systems with the University of Birmingham, Birmingham, U.K., and Director of Smart Grid, Birmingham Energy Institute. Before joining the University of Birmingham, he was an Associate Professor with the School of Engineering, University of Warwick, U.K. From 1998 to 1999, he was visiting UMIST. From 1999 to 2000, he was an Alexander-von-Humboldt Research Fellow with the University of Dortmund, Germany. He worked at China State Grid EPRI on EMS/DMS advanced application software research and development between 1993 and 1998. He is coauthor of the monograph *Flexible AC Transmission Systems: Modeling and Control* (Springer, 2006 and 2012).

Prof Zhang is an editor of the IEEE TRANSACTIONS ON SMART GRID.

Paul F. Coventry received the B.Sc. and Ph.D. degrees in electrical engineering from the University of Southampton, Southampton, U.K., in 1979 and 1984, respectively.

He joined the CEGB in 1988 and was with the Asset Management business unit of National Grid, Warwick, U.K. His work during that time focused on transmission substation plant and systems. He has managed a number of R&D projects and is currently the technical leader in HVDC technologies at National Grid.

Dr. Coventry is a Chartered Engineer in the U.K.

Ray Zhang received the Ph.D. degree in power engineering from the University of Strathclyde, Scotland.

He carried out his postdoctoral research at the University of Strathclyde, Scotland. Over last 20 years, he has been an active member of various CIGRE working groups, in 2013 he was elected as the UK Regular Member for CIGRE B5 Study Committee. Since joining National Grid, Warwick, U.K., in 1996, he has had a number of managerial and technical positions. Currently, as the Technical Leader of Protection, Control & Automation, he has the overall technical responsibility for the secondary systems within the National Grid Electricity Transmission, U.K.

Dr. Zhang is a Chartered Engineer in the U.K.